DERIVATION OF BUILDING STRUCTURES FROM NOISY DIGITAL SURFACE MODELS

Thomas Krauß

DLR, German Aerospace Center, 82234 Oberpfaffenhofen, Germany – thomas.krauss@dlr.de

KEY WORDS: Digital Twin, Building extraction, Noisy Digital Surface Models, Roof extraction, Tree detection.

ABSTRACT:

In this work we present a novel approach for segementation of a noisy DSM to building structures and other non-building structures – normally trees – and the modeling of them. Mostly Digital Surface Models (DSMs) from only a few aerial images or only from one pair of satellite images tend to be very noisy and lack good quality especially in shadow areas. Since actual methods for deriving roofs rely on a valid height information by joining areas of same slope to a roof-plane these fail regularly with such noisy DSMs. In our presented approach we use a slope map of the DSM only to detect flat regions. Since those regions on top of roofs are mostly good illuminated we can derive the ridges of roofs and flat roofs and also ground areas. All narrow, flat, elevated areas are ridges and may occur on roofs or on trees. After connecting ridges in ridge-directions there remain two types of ridges: long, straight ridges of roofs and mixed short ridges in many directions for the trees. Fitting symmetric planes through the roof-ridge-lines gives finally the roof-planes reducing the effects of noise on shadowed parts of the roof. Taking the other tree-ridges as seeds for a watershed transformation will give the trees. Finally the proposed method is applied to a noisy DSM and the results will be discussed.

1. INTRODUCTION

Creating Digital Twins (DTs) of urban areas only from Digital Surface Models (DSMs) is mostly very challenging due to (a) much noise in DSMs created only from very few stereo images like e.g. only two views for satellite imagery and (b) the intermixture of different elevated objects like buildings and trees. Due to (a) it is normally very complicated to distinguish between building and tree objects. Existing methods are mainly based on the detection of areas of homogeneous slopes for the extraction of roofs from precise DSMs like LiDAR-DSMs (Orthuber and Avbelj, 2015). But in practice in DSMs mentioned above the surface of a slanted roof on the shadowed side consists only of noise without any detectable homogeneous slope. Also LiDAR pointclouds gives the great advantage in delivering first- and last-pulse information, which allows a easy discrimination of solid objects like buildings and vegetation like trees.

Previous works rely mostly on high quality DSMs like provided with aerial laser scanning as shown in (Brenner, 2003), (Rottensteiner and Briese, 2002), (Haala and Kada, 2010) or (Perera et al., 2012). Further analysis also including other urban objects like trees are discussed in (Haala and Brenner, 1999) or for discrimination of trees and buildings using also the RGB-images as in (Krauß, 2019). The newest methods incorporate deep learning methods and are mostly based on fusing height information from DSMs with image data like in (Partovi et al., 2017).

Deeper analysis of the available noisy airborne DSMs reveals interesting details in derived filtered slope-maps: Due to the noise mainly originating from matching errors in dark, shadowed regions, bright areas like flat roofs or the ridges of gabled roofs are very stable areas and such the derived slopes in these areas are also much more reliable than those from shadowed areas. So the here presented method is based on the extraction of flat areas from noisy DSMs.

2. METHOD

The presented method consists of four main parts which are described in detail in the following sub-sections:

1. Preprocessing
2. Classification of flat areas
3. Modeling of slanted roofs
4. Modeling of trees

2.1 Preprocessing

For segmentation of a noisy DSM to building structures and other non-building structures – normally trees – we start with a preprocessing which gives us beneath the noisy DSM also a smooth DTM – a digital terrain model – representing the ground of the area as shown in fig. 1.

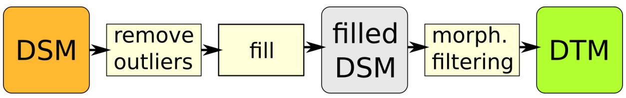

Figure 1. Preprocessing of the DSM and derivation of a DTM (images and elevation models are depicted as rounded squares, processing steps as rectangles)

Due to the noise in the DSM there are also many negative outliers below the ground surface. Hence approaches deriving a DTM from the "lowest neighbours" fail in this case dramatically. So we developed a method incorporating an outlier filtering to remove too extreme values in the noisy DSM. For the outlier filtering used in this work we calculate a mean- (μ) and standard-deviation-image (σ) of the noisy DSM using a filter radius of 2.0 m (with the given ground sampling distance (GSD) of 10 cm of the images this is a filter size of 41 px). Afterwards all DSM values lower than $\mu - \sigma$ or higher than $\mu + 2\sigma$ are removed and interpolated from neighbours as shown in fig. 2. The resulting filtered DSM is changed too heavy for further processing but perfect to derive the DTM.

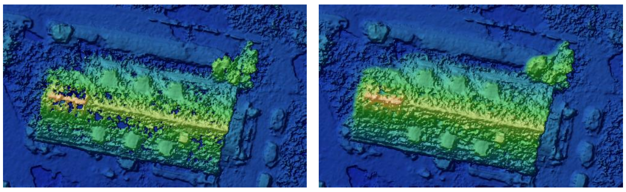

Figure 2. Detail of Dankeskirche at Tostmannplatz, Braunschweig: left: unfiltered noisy DSM, right: outlier-filtered DSM

For deriving the DTM from the outlier-filtered DSM we use the improved classical morphological approach as described in (Krauß et al., 2011). The combination of a low percentile filter (5 %) followed by a heigh percentile filter (95 %) resembles a more robust morphological opening. For both a filter radius of 100 m is used. From this DTM and the DSM a so called normalized digital elevation model or nDEM can be derived as $nDEM = DSM - DTM$ as shown in fig. 3.

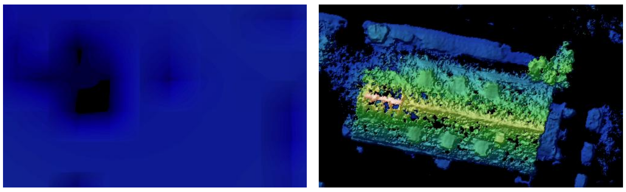

Figure 3. Same detail region as in fig. 2, left: derived DTM, right: nDEM containing only elevated objects

2.2 Classification of flat areas

The second step in our processing chain extracts and classifies flat areas in the DSM as shown in fig. 4. First a slope/aspect map is calculated from the pre-filtered DSM. To pre-filter the DSM a median filter with a window-size of 5 is applied to level out the noise, followed by a Gaussian filter with $\sigma = 2.0$. The results show low slope areas on flat roofs and on ridges of slanted roof buildings. Extracting all areas with slopes below $10°$ gives us the candidates of flat areas and the others ("*slanted*"). Using the DSM and the previously derived DTM we can calculate a so called normalized DEM (nDEM) which contains the heights of objects above ground. Using this nDEM allows us to separate high flat areas from such on the ground ("*flat low*") using a height threshold of $h = 2.5$ m.

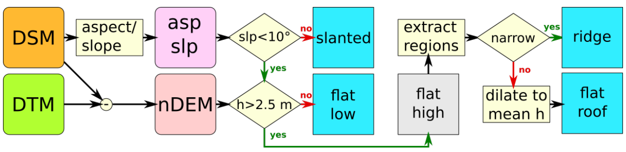

Figure 4. Classification of the DSM to flat areas, the derived class-maps fitting on the DSM are shown as cyan squares

The high flat (fig. 5) areas are further subdiveded to "*ridges*" if the detected flat area is elongated and narrow (red in fig. 5, right) and "*flat roofs*" otherwise (white in fig. 5, right). The decision which flat area is low or high is based on the nDEM and a height threshold of e.g. 2.5 m. So all flat areas below 2.5 m will become "low flat", the others "flat high" or "ridges". To distinguish between narrow and not narrow high areas a binary opening with a structuring element of a small size like e.g. 50 cm is applied. Ridges will vanish after the binary opening, larger areas will still remain.

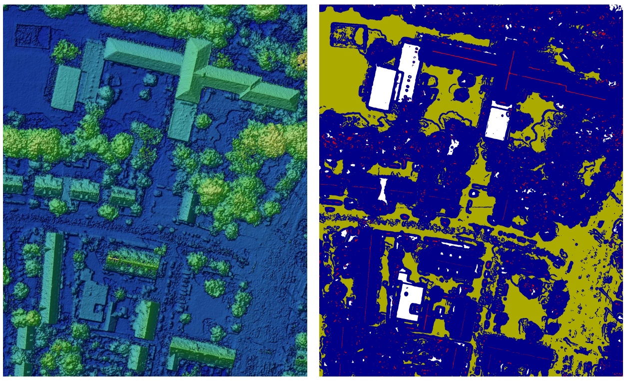

Figure 5. Classification of the DSM to flat areas, left: DSM, right: derived flat classes (blue: not flat, sand: flat low, white: flat high, red: narrow flat and high, ridges)

The flat roofs can directly be modeled at this step. For this we apply iteratively a binary dilation and add all dilated pixels to the flat roof if their height is in a small threshold (e.g. 25 cm) around the mean height of the original flat high area. The iteration stops if no more pixel could be added.

The result of this first step are flat areas of the three types "*flat low*", "*flat high*" and "*ridges*".

2.3 Modeling of slanted roofs

Afterwards we can derive the 3D vector models from the classified "*ridges*" as shown in fig. 6. It starts with the transformation of a bitmap-ridges-map to a vectorized skeleton of all ridges as shown in fig. 7, center.

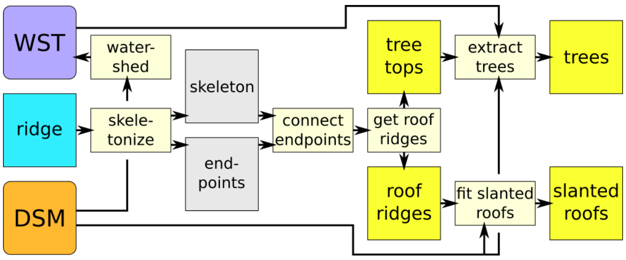

Figure 6. Modeling of slanted roofs and trees (vector objects are shown as yellow squares)

Connecting ridge areas with neighbours of same orientation and height and lying in the correct direction allows for joining of discontinous ridge areas. The result is a graph containing all connected ridge-lines of one object (see fig. 7, right). Since we have a noisy DSM many of these ridge-lines will be only small sections continuing after a missing part, so the connecting step is mandatory.

Here an other quality check occurs by checking the consistency of the height values along these extracted 3D ridge lines. Getting the roof ridges classifies the graphs to real roof-ridges (a

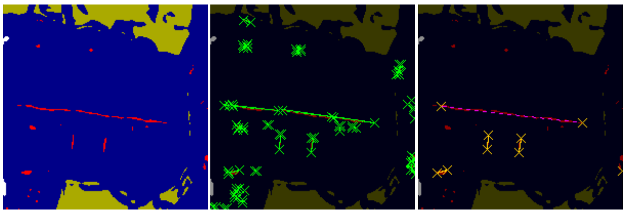

Figure 7. Skeletonization of ridges, left: class image with ridges in red, center: extracted skeleton, right: joined graph

few long, straight or rectangular lines in the graph) and tree-ridges (many small ridges in random directions). The tree-ridges are removed from the roof-ridges.

For the remaining roof-ridges profiles perpendicular to valid ridge lines are extracted and merged along each straight skeleton-vector to build up the slanted roof from planes on both sides of the ridge. Therefore height profiles parallel to the ridge line in a distance x_i are extracted until the median of the height profile is lower than the DTM plus the height-threshold or the step from the previous to the actual profile is positive (raising again) or negative and steeper than 1 m. These extracted height values for the planes are fitted through the roof-ridge-line to give the slant angle of the slanted roof.

We minimize for this the errors of a linear function $y_i = ax_i + b$ with y_i as the measured heights from the DSM and x_i the perpendicular distances to the ridge line. a gives the slope, b the offset fixed to the mean height of the ridge-line. So we will have to minimize eq. 1 for a general fixed point (x_{fix}, y_{fix}) giving $b = y_{fix} - ax_{fix}$ (in our special case the ridge line is defined as $x_{fix} = 0$ and y_{fix} as the mean height of the ridge line).

$$\varepsilon = \sum_i (ax_i + b - y_i)^2 \quad \text{or} \tag{1}$$

$$\varepsilon = \sum_i (a(x_i - x_{fix}) + (y_{fix} - y_i))^2 \tag{2}$$

The minimum of the error ε will be given by using a value of a which can be calculated from the derivative with respect to a of eq. 1 as shown in eq. 3.

$$\frac{\partial}{\partial a} \sum_i (a(x_i - x_{fix}) + (y_{fix} - y_i))^2) = 0 \quad \text{or} \tag{3}$$

$$a = \frac{\sum_i (y_i - y_{fix})(x_i - x_{fix})}{\sum_i (x_i - x_{fix})^2} \tag{4}$$

So we have finally fitted two planes – left and right – through the ridge line with the common length of the ridgeline l, a individual width $w_{l,r}$ and slope $a_{l,r}$. Now these planes undergo a quality assessment. First the planes should have a width of more than 1 pixel and they should not be wider than 1.2 times the length of the ridge. Second the planes should be about the same width (one plane not being smaller than 0.2 the width of the other plane). Third the values for the slopes a of the planes left and right of the ridge should not differ more than 10° and both should be larger than 10° going downward (not flat and descending).

If all these quality checks are passed the planes are reduced to the minimum width of both ($w = \min(w_l, w_r)$) and the slopes are set to the mean of the both slopes ($a = (a_l + a_r)/2$). Finally the four corners of each plane are derived as the two ridge-points at mean ridge-height H and the two eaves points at the height of the eaves derived from the plane width and slope as $h_{l,r} = H + aw$. The result for the region shown in fig. 7 is given in fig. 8.

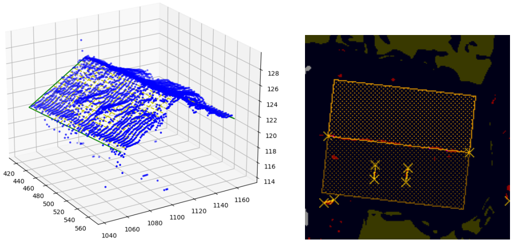

Figure 8. Resulting fitted roof, left: 3D view of points (blue dots) and fitted planes (yellow grid), right: resulting harmonized and fitted roof (. . . with remaining two small ridges of unmodeled dormers)

2.4 Modeling of trees

To model the trees first a inverted watershed-transformation (Beucher, 1982, Haithcoat et al., 2009) is applied to the Gaussian filtered ($\sigma = 5.0$) noisy DSM providing a segmentation by the local maxima as shown in fig. 6, upper part and in fig. 9, left.

For each of the watershed segments a high-mask (e.g. with a height of 4 m above the DTM) is calculated. If the class "not flat" dominates this high-mask it is taken as a tree. The center of gravity gives the trunk position. Using the area A of the high mask gives the radius of the tree as $r = \sqrt{A/\pi}$. The height of the tree is given by the nDEM height at the tree position.

The derived trees (and buildings) are shown in fig. 9, right.

3. EXPERIMENTS

3.1 Data

The method is applied to a noisy DSM from a flight campaign over Braunschweig which was flewn on 2020-07-31 from 9:30 to 11:30. As test area an area of 180×220 m^2 around the Tostmannplatz is selected as shown in fig. 5, left. The corresponding result is shown in fig. 9, right.

4. DISCUSSION

As can be seen the result of the presented method shown in fig. 9 gives alread very good results. Most of the buildings are modeled correctly, the tree areas are also mapped correctly. But some problems and possible improvements to the method can be seen. Following points are worth remarking:

- Hipped roof parts are often missed or wrongly detected
- Problems with complicated roofs like at the large building at the top
- The method cannot detect a roof if no flat ridge exists (left part of the church slightly below the center of the image is modeled as group of trees)

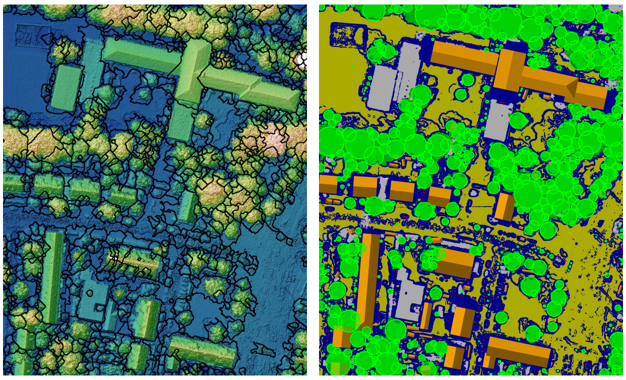

Figure 9. Results of the presented method based on the test area, left: DSM segmented using the watershed-transformation, right: results (buildings and trees as vector-objects, remaining classes: gray: flat roofs, sand: low flat areas, blue: not flat areas)

- The vectorization of flat roofs is still missing
- Dormers are missing
- Some small areas are wrongly detected as flat or slanted roofs
- A correct joining of roof-parts is still missing (e.g. the building in the lower right edge)

5. CONCLUSIONS AND OUTLOOK

In this paper we presented a method to derive building- and tree-objects from only a noisy digital surface model (DSM). The process derives from a noisy DSM a digital terrain model (DTM), flat roof areas, slanted roof areas, trees and low flat areas. The first results of this work look very promising but there is still some further research needed.

Future work should include the vectorization of the flat roof areas and the proper detection of hipped roofs and dormers. Afterwards also a correct intersection of all detected roof planes should be implemented. Also the mis-classification of small areas to flat or slanted roofs should be solved.

REFERENCES

Beucher, S., 1982. Watersheds of Functions and Picture Segmentation. *IEEE International Conference on Acoustics, Speech and Signal Processing*, 1928–1931.

Brenner, C., 2003. Building Reconstruction from Laser Scanning and Images. *ITC Workshop on Data Quality in Earth Observation Techniques*.

Haala, N., Brenner, C., 1999. Extraction of buildings and trees in urban environments. *ISPRS Journal of Photogrammetry & Remote Sensing*, 54, 130–137.

Haala, N., Kada, M., 2010. An update on automatic 3D building reconstruction. *ISPRS Journal of Photogrammetry and Remote Sensing*, 65(6), 570-580.

Haithcoat, T., Song, W., Hipple, J., 2009. Automated Building Extraction and Reconstruction from LIDAR Data. Technical report.

Krauß, T., 2019. Deriving leafless trees and urban structures from the DLR 3K airborne camera system for the city of Braunschweig. *Proc. SPIE*, 11174, 1-8.

Krauß, T., Arefi, H., Reinartz, P., 2011. Evaluation of selected methods for extracting digital terrain models from satellite born digital surface models in urban areas. *International Conference on Sensors and Models in Photogrammetry and Remote Sensing (SMPR 2011)*.

Orthuber, E., Avbelj, J., 2015. 3D Building Reconstruction from LiDAR Point Clouds by Adaptive Dual Contouring. *ISPRS Annals of the Photogrammetry, Remote Sensing and Spatial Information Sciences*, II/3/W4, 157–164.

Partovi, T., Fraundorfer, F., Azimi, S., Marmanis, D., Reinartz, P., 2017. Roof type selection based on patch-based classification using deep learning for high resolution satellite imagery. *International Archives of the Photogrammetry, Remote Sensing and Spatial Information Sciences*, XLII(1/W1), 653-657.

Perera, S. N., Nalani, H. A., Maas, H. G., 2012. An automated method for 3D roof outline generation and regularization in airbone laser scanner data. *ISPRS Annals of the Photogrammetry, Remote Sensing and Spatial Information Sciences*, I(3), 281-286.

Rottensteiner, F., Briese, C., 2002. A New Method for Building Extraction in Urban Areas from High-Resolution Lidar Data. *International Archives of Photogrammetry and Remote Sensing*, XXXIV / 3A, 295–301.